Tempering Temperature and Blunt Notch Fracture Toughness of Ni-Cr-Mo Steels

D. FIRRAO*, R. ROBERTI**, G. M. LA VECCHIA**
*Dipartimento di Scienza dei Materiali e Ingegneria Chimica, Politecnico di Torino, C. so Duca degli Abrizzi, 24, Torino, Italy.
**Dipartimento di Chimica-Fisica Applicata, Politecnico di Milano, P. zza Leonardo da Vinci, 32, Milano, Italy

ABSTRACT

To interpret ductile fractures of steels, several models of micro-mechanisms have been developed and quantitative relationships between the macroscopic properties and the microstructural features proposed.
Recently Firrao and Roberti, describing the phenomena intervening during the process of ductile fracture nucleation and subsequent propagation in mild steels, have introduced a mathematical relationship, derived by one proposed by Rice, which takes into account the J-integral applied to a blunt notch specimen, the notch-end radius, the strain hardening properties of a material and the maximum strain acting at the notch root.
It was demonstrated that the limiting value of the radius of curvature achieved by the crack tip during blunting is directly related to the interparticle spacing between large inclusions, whereas the maximum strain acting at the notch root at the onset of fracture propagation is strongly dependent on the total second phase particles volume fraction.
In the present research experiments have been conducted on a 0.39% C quenched and tempered Ni-Cr-Mo steel to study the influence of micro-structure, inclusions and notch root radius values on the macroscopic toughness.
The obtained results have allowed to further validate the procedure of J_{Ic} determination based on fracture toughness testing of non pre-cracked specimens and quantitative metallographic analysis of the material structure.
The role of non metallic inclusions and carbides in governing the ductile fracture development processes has been clarified: the former control the blunting process while the latter play a role in promoting the fracturing of remaining ligaments between first nucleated pores.

KEYWORDS

Ductile fracture, ductile fracture models, J-integral, notch root radius, fracture micromechanisms , 2nd phase particles, inclusions.

INTRODUCTION

The critical role of inclusions in ductile fractures has long been recognized since they act as nucleating agents of the micropores which lead to the development of the final dimpled rupture surfaces. Physical and mathematical models which take into account their size, interpartical distance and volume fraction to interpret fracture toughness data have been developed by various authors (Firrao et al., 1984).

In the case of quenched and tempered steels the role of inclusions has been seen as antagonized by the effect of carbides formed during the final stage of tempering (Cox et al., 1974). The relative importance of each category of the above 2nd phase particles has not been clearly singled out. Therefore, this class of steels has often eluded an adequate modelling due to the fact that no general ductile fracture model has been recognized applicable to the accurate prediction of their fracture toughness properties (Schwalbe, 1977; Slatcher et al., 1981). Only Ebner and Maurer (1982) have found a correlation between the prediction based on the model developed by Hahn and Rosenfield (1968) and the experimental results on a 0.32% C, 1.5% Cr, 1.5% Ni steel quenched and tempered between 450 and 650 °C.

The critical analysis of models proposed up to now (Firrao et al., 1984) has led to the conclusion that they are not able to yield accurate predictions if applied both to mild or quenched and tempered low alloy high strength steels, also because the application to each case requires the determination of the univocal weight of the influence of the various 2nd phase particles distribution parameters.

A new promising model describing the phenomena intervening during the process of ductile fracture nucleation and extension from a pre-existing crack in mild steel components has been recently proposed by the authors (Roberti et al., 1986).

It encompasses several stages under increasing applied stresses: (i) initial crack-tip blunting and void nucleation around first-row large second-phase particles, (ii) increase of the radius of curvature of the blunted tip up to a limiting value and concurrent joining of the crack-front to first-row enlarged voids, (iii) further straining of the remaining ligaments between voids already connected to the crack front up to their rupture that marks the final overall crack advance.

It follows that the level of fracture toughness (J_{Ic}) in mild steels is in effect determined by the amount of plastic yielding intervening in stages (ii) and (iii) at the stress concentration prior to the ligament failure; next, the extension of such a deformation process is in turns governed by the microstructural features of the steel. In fact, as regards stage (ii), the limiting value of the radius of curvature achieved by the crack-tip during blunting is almost identical to the spacing among major inclusions. The resistance to the real crack advance (stage iii) is then determined by the capacity of the matrix material between pores to continue to flow up to a limiting fracture strain. The level of such a property is enhanced by the ability of the matrix to strain-harden and is foreshortened by its tendency to strain localization; it therefore depends on the total 2nd phase particles volume fraction and the local state of stress.

The above described physical model has led the authors (Firrao et al., 1984; Roberti et al., 1986) to the following mathematical formulation for ductile

fracture toughness,

$$J_{Ic} = \sigma_y^{(1-N)} \cdot \varepsilon^{*(1+N)}_{max,f} \cdot E^N \cdot \underline{s}/F(\Gamma(N)) \qquad (1)$$

Eq.1 has been derived from the mathematical relationship proposed by Rice (1968) among the J-integral applied to a blunt notch specimen, the notch-end radius, ρ, the strain hardening properties of a material, N, and the maximum strain acting at the notch root, ε^*_{max},

$$\varepsilon^*_{max} = \varepsilon_y \cdot \{[F(\Gamma(N)) \cdot J]/[\sigma_y \cdot \varepsilon_y \cdot \rho]\}^{1/(1+N)} \qquad (2)$$

If the maximum strain acting at the notch root at fracture initiation is always the same whichever the value of ρ, the above equation becomes a criterion for ductile fracture and can be written,

$$\varepsilon^*_{max,f} = \varepsilon_y \cdot \{[F(\Gamma(N)) \cdot J_A]/[\sigma_y \cdot \varepsilon_y \cdot \rho]\}^{1/(1+N)} \qquad (3)$$

where J_A is the value of the J-integral applied at fracture nucleation in a blunt notch specimen.

For a given material, Eq.3 depicts a straight line passing through the origin of the J_A-ρ field, with its angular coefficient being a function of $\varepsilon^*_{max,f}$. For ρ's smaller than a limiting value the above equation loses its physical meaning. Such a limiting value, usually referred to as ρ_{eff}, is the maximum notch-end radius that causes a notched specimen to fail at the same level of fracture toughness as pre-cracked test-pieces of the same material. From what has been said before, ρ_{eff} coincides with $\underline{s}$. Thus, experiments on notched specimens with $0 < \rho < \underline{s}$ allow to determine the level of J_{Ic} of the material, whereas tests on samples with $\rho > \underline{s}$ provide the inclination of the above referred sloped line from which $\varepsilon^*_{max,f}$ can be eventually derived.

Test results on C-Mn ferritic-pearlitic steels have confirmed the above and permitted to assess that the mathematical model described by Eq. 1 is able to foresee the fracture toughness of a mild steel after performing quantitative metallography to determine the value of $\underline{s}$, as well as fracture mechanics tests on notched samples with a specific ρ value. In fact, the combination of Eqs.1 and 3 leads to,

$$J_{Ic} = (J_A/\rho) \cdot \underline{s}. \qquad (4)$$

Furthermore, experiments performed with samples with varying notch root radii allow to single out which is the value of ρ_{eff} relevant to a steel in a given metallurgical condition. Therefore, the above described model allows to ascertain which are the 2nd phase particles which play the most significant role in the ductile fracture development process.

To extend the applicability of the above described physical-mathematical model to the prediction of fracture toughness data of quenched and tempered low alloy high strength steels, as well as to pinpoint which are the 2nd phase particles controlling their fracture, it has been decided to initiate an articulate research program; it is intent to measure fracture toughness properties of various heats of the same class of Ni-Cr-Mo steels, quenched and tempered at increasing temperatures selected in order to be sure that the fracture process is fully ductile.

Results pertaining to the first heat of UNI 39 NiCrMo 3 steel quenched and tempered at 550, 600, and 650 °C are hereby presented.

MATERIAL AND EXPERIMENTAL PROCEDURE

Table I reports the chemical composition of the UNI 39 NiCrMo 3 steel used in the investigation; the steel had been produced in an electric arc furnace, with no subsequent ladle treatment.

Table I. Chemical composition (wt.%) of the UNI 39 NiCrMo 3.

C	Mn	Si	P	S	Cr	Ni	Mo	Cu	Sn	Al	O	N
.42	.72	.27	.018	.008	.90	.84	.17	.22	.023	.016	.0033	.010

Three point bending specimen blanks were machined in the LT direction, with a thickness B = 20 mm.
Austenitizing was done at 850 °C for 1 h, followed by oil quench and then tempering at 550, 600, and 650 °C for 3 h.
Longitudinal tensile properties are reported in Table II.
After final surface grinding notches with different end radii were machined in the bending specimens; ρ values were selected in the range between 0.21 and 0.76 mm in order to have notch root radii both smaller and larger than the mean interparticle spacing. Some specimens were also fatigue precracked.

Fracture mechanics tests were carried out by means of a 100 kN INSTRON mod. 1195, at a cross head speed of 0.0083 m/s. J_{Ic} values were determined according to the ASTM E 813-87 standard, with the unloading compliance method to generate the J resistance curves. J_A values at initiation for the blunt notch specimens were determined at the intersection between the ordinate axis and the linear regression line that fits the experimental points.
No J resistance curves were obtained for samples tempered at 550 °C since fracture initiation was immediately followed by unstable propagation, therefore J_{Ic} and J_A values were obtained at the load drop on the autographic load-deflection plot.

Table II. Longitudinal tensile properties as a function of tempering temperatures.

Tempering Temperature [°C]	σ_{UTS} [MPa]	σ_y [MPa]	Elongation [%]	Reduction of Area [%]	Strain hardening exponent, N
550	1179	1110	10	43.8	0.063
600	1049	922	18	43.3	0.071
650	865	757	24	55.3	0.084

Quantitative metallography of non metallic inclusions was carried out by means of a Bausch & Lomb, Omnicon Alpha, image analyzer. An ISI S IIIA scanning electron microscope was used for microfractographic examinations of the fracture surfaces.

RESULTS

Upon tempering the martensite packets progressively loose their lath structure; precipitating carbides become larger and tend to spheroidize. Maximum equivalent diameter of carbides was 0.4 μm in the 650 °C tempering condition; their interparticle spacing increased passing from 550 to 650 °C tempering temperature (approximately in the range .3 - .7 μm).

Relevant inclusion distribution parameters are: the interparticle spacing, s, in the crack propagation plane and the average equivalent diameter, D, on the same plane, which, in the case in study, is perpendicular to the rolling direction. Of importance is also the total volume fraction, f. Values of s, D and f were 290 μm, 2.5 μm and 0.056 %. Prior austenitic grain size was determined as being 18 μm.

Fractographic analysis allowed to ascertain that in all the tested metallurgical conditions a fully ductile fracture was reached. Major dimples of 100-120 μm equivalent diameter were connected by microdimpled fracture surfaces characterized by increasing deformation phenomena as the tempering temperature was raised (Fig.1).

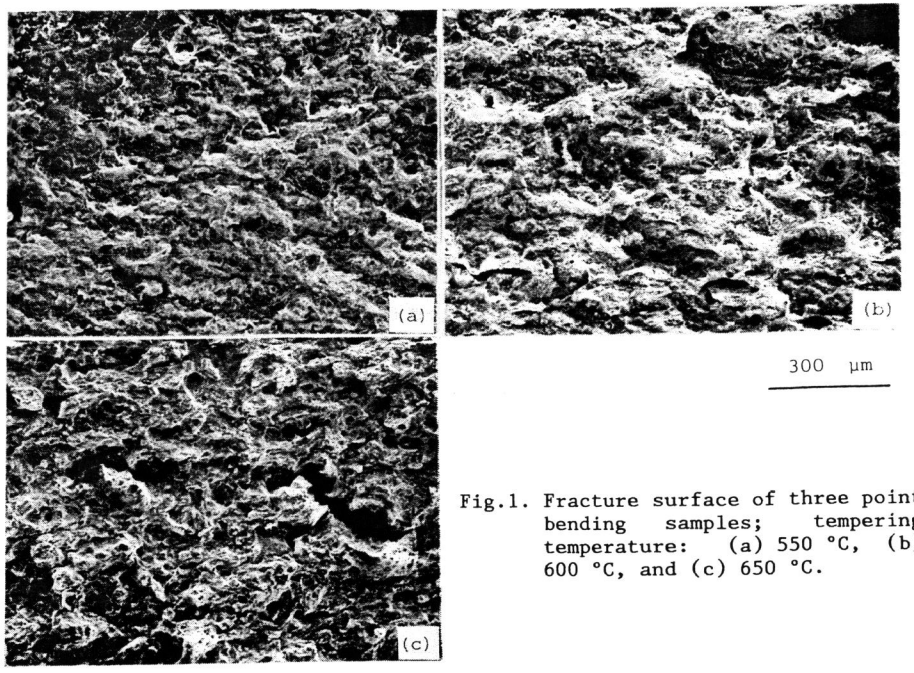

Fig.1. Fracture surface of three point bending samples; tempering temperature: (a) 550 °C, (b) 600 °C, and (c) 650 °C.

J-integral values applied at the onset of fracture both in precracked and notched three point bending specimens have been plotted in Fig.2 as a function of initial notch root radii.
dJ/da values, as determined by the regression analysis of J resistance data, resulted almost coincident either for precracked or blunt notch specimens, thus invigorating the idea that blunt notch specimens can be used to determine J_{Ic} values.

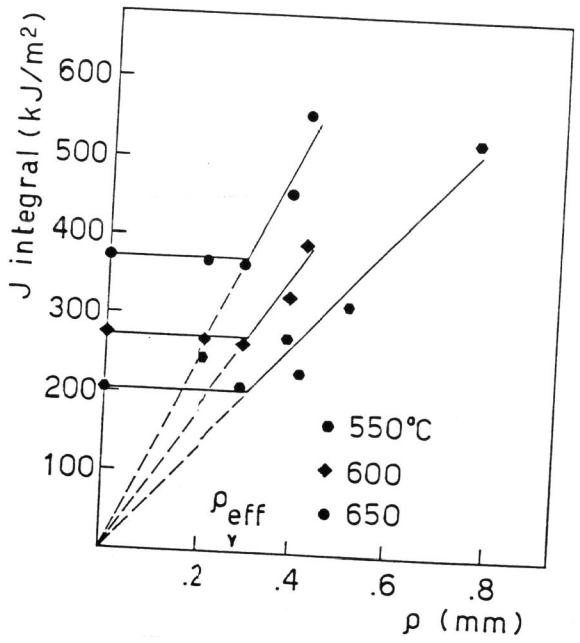

Fig.2 - J-integral values at fracture initiation as a function of notch root radius and tempering temperature.

Data plotted in Fig.2 clearly show that constant J values are met up to a limiting value of the notch root radius, as foreseen by the physical model proposed by the authors. Thereafter, fracture mechanics results interpolate to a sloped straight line passing through the origin, as expected on the basis of Eq.3.

The ρ_{eff} value, as determined by the geometrical analysis of the plot of Fig.2 is the same for the three tested metallurgical conditions and coincides with the interparticle spacing among major inclusions.

The two findings combine to discount any influence of carbides on the two

first steps (i) and (ii) in the ductile fracture development process in low alloy high strength quenched and tempered steels, if a sufficiently high tempering temperature is adopted. In fact, the value of s to be inserted in Eq.1 has resulted to be the same in the tested cases.
Instead, the role of carbides becomes progressively more important when the stage (iii) activates. At 550 °C strain hardening properties of the matrix material are too low and plastic microinstability develops in the ligaments connecting macropores, thus reducing the amount of plastic deformation that can be sustained at the crack tip prior to the final crack advance. Low values of $\varepsilon^*_{max,f}$ are then achieved.

Plastic microinstability phenomena alleviate as the matrix material softens and increases its strain hardening capacity upon increasing the tempering temperature. Thus higher values of $\varepsilon^*_{max,f}$ can be reached more than compensating the softening of the matrix in the final control of the fracture toughness (J_{Ic}), as foreseen by Eq.1.

CONCLUSION

Test results on Ni-Cr-Mo steels quenched and tempered at 550, 600, 650 °C allow to prove that in fully ductile fractures:

i) the blunting process of a preexisting crack is always governed by the distribution parameters of the non metallic inclusions. These also form the larger dimples which set the average dimension remaining ligaments of the matrix material in which further deformation phenomena take place prior to the final crack advance;

ii) precipitated carbides can act only at the final stage of the ductile fracture process in promoting the fracturing of remaining ligaments between first nucleated pores ahead of the blunted crack tip.

Furthermore, as a general conclusion, it has been proved that:

iii) fracture mechanics (J_A) tests on blunt notch specimens combined with quantitative metallography of non metallic inclusions distribution, provide an easy determination procedure of J_{Ic} values also in the case of quenched and tempered low alloy high strength steels.

REFERENCES

Cox, T.B. and Low Jr., J.R. (1974). An investigation of the plastic fracture of AISI 4340 and 18 Nickel-200 grade maraging steels. Met. Trans., 5, 1457-1470.

Ebner, R. and Maurer, K.L. (1982). Microstructure and ductile fracture in a quenched and tempered steel. In: Fracture and the Role of Microstructure, (K.L. Maurer, F.E. Matzer, eds.) pp.296-303. EMAS, Warley, U.K.

Firrao, D. and Roberti, R. (1984). On the mechanisms of ductile fracture nucleation ahead of sharp cracks. In: Fracture: Interactions of Microstructure, Mechanisms and Mechanics, (J.M.Wells, J.D.Landes, eds.), pp.165-177. The Metallurgical Society of AIME, Los Angeles, (USA).

Hanh, G.T. and Rosenfield, A.R. (1968). Sources of fracture toughness: the relationship between K_{Ic} and the ordinary tensile properties of metals. In: Application Related Phenomena in Titanium Alloys, ASTM STP 432, pp.5-32. ASTM, Phyladelphia.

Rice, J.R. (1968). A path independent integral and the approximate analysis of strain concentration by notches and cracks. J. Appl. Mech. Trans. ASME E, 35, 379-386.

Roberti, R. and Firrao, D. (1986). Physical and mathematical modelling of crack tip blunting in C-Mn ferritic-pearlitic steels. In: Fracture Control of Engineering Structures (H.C. Van Elst, A.Bakker, eds.), Vol.III, pp.2185-2194. EMAS, Warley, U.K.

Schwalbe, K.H. (1977). On the influence of microstructure on crack propagation mechanisms and fracture toughness of metallic materials. Engnr. Fract. Mech, 9, 795-832.

Slatcher, S. and Knott, J.F. (1981). The ductile fracture of high strength steels. In: Advances in Fracture Research (D.Francois, ed.), Vol.1, pp.201-207, Pergamon Press, Oxford.